Characterization of the Equilibrium $PF_4CF_{3,ax} \Leftrightarrow PF_4CF_{3,eq}$ by Matrix Isolation FTIR Spectroscopy

O. Lösking,[†] H. Willner,*[,†] H. Oberhammer,[‡] J. Grobe,[§] and D. Le Van[§]

Institut für Anorganische Chemie, Universität Hannover, 3000 Hannover, FRG, Institut für Physikalische und Theoretische Chemie, Universität Tübingen, 7400 Tübingen, FRG, and Institut für Anorganische Chemie, Universität Münster, 4400 Münster, FRG

Received December 27, 1991

Equilibrium mixtures of $PF_4CF_{3,ax} \Leftrightarrow PF_4CF_{3,eq}$ in the temperature range −125 to +120 °C have been quenched in Ar and Ne matrices. The resulting infrared spectra have been used to deduce the spectra of the pure isomers and to evaluate the equilibrium constants. The temperature dependence of the equilibrium constants yields $\Delta H° = 4.32 \pm 0.05$ kJ mol^{-1} and $\Delta S° = 15.4 \pm 1.0$ J mol^{-1} K^{-1}, with $PF_4CF_{3,ax}$ being the more stable isomer. Results from ab initio calculations at the Hartree-Fock 3-21G* level support the vibrational assignment and permit calculation of $\Delta S°$. The properties of the unusual PF_4CF_3 molecule are discussed in detail.

Introduction

Hypervalent pentacoordinated compounds with flexible molecular frameworks are of primary interest in stereochemistry. For phosphorus compounds with monofunctional substituents, PL_4X, a trigonal-bipyramidal framework is adopted. The location of the substituent X in an axial or equatorial position and the rate of ligand exchange by pseudorotation depend strongly on the nature of the ligands and substituents. The free energy difference between the axial (I) and equatorial (II) isomer is due mainly

I II

to the difference in bond energies $D(PL_{eq}–PL_{ax}) - D(PX_{eq}–PX_{ax})$ and an entropy term. The activation energy for pseudorotation is due to bond strengthening and nonbonding interactions on this reaction pathway.

Predictions of the more stable isomer by the "electronegativity rule"[1] and the concept of "apicophilicity"[2] give rise to many discrepancies as discussed earlier.[3] In this context the molecule PF_4CF_3 is of particular interest, because an electron diffraction study deduced a mixture of both isomers (equatorial/axial), in the ratio 6:4.[3] Previous structural studies on PF_4CF_3 were contradictory. From ^{19}F-NMR chemical shifts[4] and from a microwave study[5] at low temperature, it was concluded that the CF_3 group occupies an axial position (I). On the other hand ^{13}C NMR data[6] and gas-phase infrared spectra[7] implied an equatorial isomer (II). MO calculations at the CNDO/2 level[8] result in a difference of 96 kJ mol^{-1} for the bond energies, favoring clearly the equatorial isomer (II).

At the same time as the electron diffraction study,[3] the equilibrium mixture (axial/equatorial) of PF_4CF_3 quenched in an argon matrix was investigated by infrared spectroscopy by H.W. (in 1981). In the infrared matrix spectrum both isomers were clearly observable. But the study was not completed, due to insurmountable problems caused by hydrolysis and determination of relative integrated band intensities. Now with better sample-handling techniques and better instrumentation (FTIR) the study was repeated to measure vibrational data for both isomers, to determine the equilibrium constant as function of temperature, and to identify the more stable isomer and evaluate the enthalpy difference.

Experimental Section

Synthesis. (Trifluoromethyl)tetrafluorophosphorane, PF_4CF_3, was prepared by a modified literature procedure.[9] Halogen exchange of PI_2CF_3 to PF_2CF_3 was achieved with freshly sublimed antimony trifluoride at 30–50 °C within 48 h in a glass vessel. Further fluorination ensued by use of XeF_2. Thus, about 1 g of XeF_2 (ca. 6 mmol) was placed in a PFA reactor (volume ca. 100 mL) equipped with a PFA valve (Galtek type 201–10, Fluoroware Inc., Chaska, USA). Approximately 3 mmol of PF_2CF_3 was added in vacuo, and the reaction proceed to completion after 50 min at 0 °C. Purification of the product was carried out in vacuo by fractional condensation between traps held at −127, −150, and −196 °C. The middle fraction (PF_4CF_3) was checked for purity by infrared and ^{19}F NMR spectroscopy. Traces of $CF_3P(O)F_2$ (<1%) were the only detectable impurity. The yield based on PF_2CF_3 is more than 90%; byproducts are PF_5, and $PF_3(CF_3)_2$.

Because PF_4CF_3 is easily hydrolyzed, the glass vacuum line was dried with $SOCl_2$ prior to use.

Recording of Spectra. Raman spectra of liquid PF_4CF_3 were recorded in the temperature range −100 to −20 °C using a Coderg T 800 instrument equipped with an Ar^+ ion laser (Spectra Physics, 514.5 nm, 500 mW). The temperature of the sample, flame-sealed in a thin-wall 5-mm NMR tube, was maintained by a stream of cold nitrogen gas and measured by an Pt-100 sensor placed beside the sample on the wall of the NMR tube. Matrix infrared spectra were measured on a IFS 66v FTIR spectrometer (Bruker, Karlsruhe, FRG) operating in reflection mode in the range 4800–80 cm^{-1} with an apodized resolution of 1 cm^{-1}. In the wavenumber ranges above and below 400 cm^{-1} two different DTGS detectors were used and 128 and 64 scans respectively were summed. Gas phase infrared spectra were obtained using a MX-1 FTIR spectrometer (Nicolet, Offenbach, FRG) operating in the range 4800–400 cm^{-1} with a resolution of 4 cm^{-1}. Samples were contained in a 17-cm glass cell equipped with IR grade silicon windows (Wacker-Chemie, Burghausen, FRG).

* To whom correspondence should be addressed.
† Universität Hannover.
‡ Universität Tübingen.
§ Universität Münster.

(1) Gillespie, R. J.; Nyholm, R. S. *Chem. Soc. Rev.* **1975**, *11*, 339. Gillespie, R. J. *Can. J. Chem.* **1960**, *38*, 818. Gillespie, R. J. *J. Chem. Educ.* **1970**, *47*, 18.
(2) Ugi, I.; Marquarding, D.; Klusacek, H.; Gillespie, P.; Ramirez, F. *Acc. Chem. Res.* **1971**, *4*, 288.
(3) Oberhammer, H.; Grobe, J.; Le Van, D. *Inorg. Chem.* **1982**, *21*, 275.
(4) Muetterties, E. L.; Mahler, W.; Schmutzler, R. *Inorg. Chem.* **1963**, *2*, 613.
(5) Cohen, E. A.; Cornwell, C. D. *Inorg. Chem.* **1967**, *7*, 398.
(6) Cavell, R. G.; Gibson, J. A.; The, K. I. *J. Am. Chem. Soc.* **1977**, *99*, 7841.
(7) Griffiths, J. E. *J. Chem. Phys.* **1968**, *49*, 1307.
(8) Gillespie, P.; Hoffman, P.; Klusacek, H.; Marquarding, D.; Pfohl, S.; Ramirez, F.; Tsolis, E. A.; Ugi, I. *Angew. Chem.* **1971**, *83*, 691; *Angew. Chem., Int. Ed. Engl.* **1971**, *10*, 687.
(9) Mahler, W. *Inorg. Chem.* **1963**, *2*, 230.

0020-1669/92/1331-3423$03.00/0

Table I. Measured and Calculated Fundamental Wavenumbers (cm^{-1}) of $PF_4CF_{3,ax}$

IR spectrum[a]			Raman spectrum			calc[d]		
Ne matrix	Ar matrix	int[b]	liq	int	ρ[c]	value	int (IR)	assignt (C_{3v}); approx descrpn of mode
1244.4	1243.5	13	1236	w	0.7	1271	7.7	a_1; $\nu_s(CF_3)$
1179.7	1174.9	100	1170	w		1247	68.2	e; $\nu_{as}(CF_3)$
985	979	96	985	w, br	dp	1040	49.8	e; $\nu_{as}(PF_{3,eq})$
887	885	73	880	w, br	0.4	957	100	a_1; $\nu(PF_{ax})$
			752	s	0.3	767	0.6	a_1; $\nu_s(PF_{3,eq})$
712.5	712.3	7	713	w	0.6	692	1.4	a_1; $\delta_s(CF_3)$
577.5	576.1	18	577	sh	(p)	560	45.6	a_1; $\delta_{oop}(PF_{3,eq})$
	555.7	0,7	557	m	dp	520	0.2	e; $\delta_{as}(CF_3)$
	509	7	509	w	dp	487	7.5	e; $\delta_{as}(PF_{3,eq})$
	385.0	3	385	m	dp	367	2.5	e; $\rho(CF_3)$
	302.9[e]		303	m	0.4	303	0.3	a_1; ν(P-CF_3)
	225	2	228	w	dp	212	2.2	e; $\rho(PF_4)$
			138	w	dp	123	1.0	e; $\delta(PF_4$-$CF_3)$
						77	0	a_2; $\tau(CF_3)$

[a] Average over matrix splittings. [b] Relative integrated band intensity. [c] Polarization ratio. [d] Ab initio calculations (HF/3-21G*); wavenumbers normalized by a factor of 0.9. [e] Measured only in the spectrum of the neat solid at 100 K.

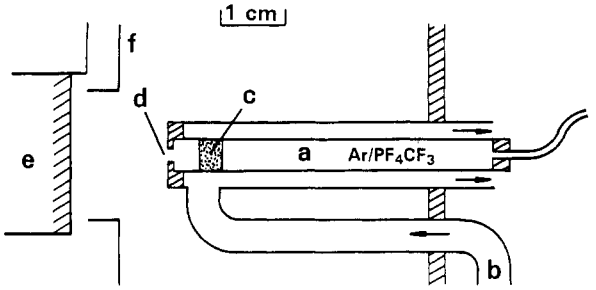

Figure 1. Nozzle for attainment of the $PF_4CF_{3,ax}/PF_4CF_{3,eq}$ equilibrium at different temperatures: (a) chamber, temperature controlled by a flow of nitrogen from tube b; (c) porous stainless steel frit; (d) orifice; (e) matrix support; (f) radiation shield (77 K).

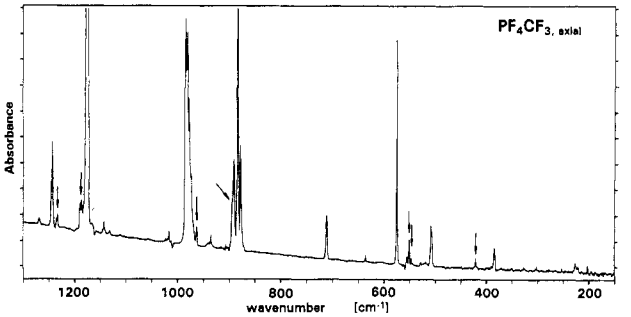

Figure 2. Infrared spectrum of $PF_4CF_{3,ax}$ isolated in an argon matrix, calculated from the spectrum of an equilibrium mixture (sample: Ar = 1:1000; 0.7 mmol matrix) at −125 °C minus that at +120 °C. Arrows indicate bands due to the impurity $PF_2(O)CF_3$.

Isolation of the Equilibrium Mixture $PF_4CF_{3,ax}/PF_4CF_{3,eq}$ in Noble Gas Matrices. Prior to use, the stainless steel vacuum line, transfer capillary, and temperature-controlled nozzle (Figure 1) of the matrix isolation apparatus were dried with ClF_3 and passivated with PF_4CF_3. With such precautions, mixtures of PF_4CF_3/Ar(Ne) 1:1000 can be stored in the vacuum line for days without any decomposition. Amounts of gas mixtures deposited as a matrix were determined from the known volume (1094.3 mL) of the vacuum line and the temperature and pressure of the gas. The presssure was measured by a Setra 280 E capacity manometer (pressure range 0–1700 mbar; resolution 0.1 mbar). The gas flow into the temperature-controlled nozzle and the cryostat (Figure 1), of exactly 1.50 mmol/h in all experiments, was adjusted by a needle valve. Under these conditions the Ar pressure in the temperature-controlled chamber (a) of 1.7-mL internal volume is about 30 mbar. The complete nozzle assembly is placed in the high vacuum system ($p < 10^{-7}$ mbar) of the matrix cryostat and is heated or cooled by a stream of nitrogen, which enters via tube b. A Pt-100 temperature sensor is fitted near (c) in the nitrogen gas stream. In the stainless steel frit (c) of 5-mm thickness and 0.2-mm porous diameter the pressure of 30 mbar is slowly reduced to a few millibar. Finally the gas mixture emerges from the orifice (d) and is quenched as a matrix on the support (e). As discussed later, the equilibrium $PF_4CF_{3,ax}/PF_4CF_{3,eq}$ is attained completely at all temperatures used. The matrix support (e) is a highly reflecting aluminum-covered, nickel-plated copper block that is cooled for Ar (Ne) matrices down to 11 K (5 K) by the aid of a liquid helium continuous flow cryostat (Cryovac, Troisdorf, FRG). For 20 Ar matrix experiments nozzle temperatures of about +120, +80, +20, −20, −90, and −125 °C were used for sample amounts in the range 0.4–2 mmol. In each of two Ne matrix experiments the nozzle temperature was +120 and −125 °C, respectively.

Results and Discussion

Vibrational Spectra of the PF_4CF_3 Isomers. Infrared spectra obtained from the equilibrium mixtures at the highest (+120 °C) and lowest temperature (−125 °C) used

$$PF_4CF_{3,ax} \rightleftharpoons PF_4CF_{3,eq} \quad (1)$$

quenched in argon matrix exhibit the greatest differences. The spectra measured at these extremes of temperatures have been analyzed to yield the spectra of the pure isomers by spectra substraction, with the results shown in Figure 2 and Table I (low-temperature species) and in Figure 3 and Table II (high-temperature species). Raman spectra of the liquid compound were measured in the temperature range −100 to −20 °C, just above the melting (−117 °C), and boiling (−35 °C) points.[9] At these temperatures the low-temperature species is predominant (see determination of equilibrium), and only a few Raman lines of the high-temperature species could be identified. The Raman wavenumbers of both isomers are included in Tables I and II. The symmetry of the axial isomer (I) is C_{3v} and that of the equatorial isomer (II) is C_{2v} if we assume free internal rotation of the equatorial CF_3 group. Accordingly, the irreducible representations for the 21 fundamental vibrations are as follows:

$$\text{(I) } C_{3v}\text{: } \Gamma_{vib} = 6a_1\ (\text{IR, Ra p}) + a_2\ (-, -) + 7e\ (\text{IR, Ra dp})$$

$$\text{(II) } C_{2v}\text{: } \Gamma_{vib} = 7a_1\ (\text{IR, Ra p}) + a_2\ (\text{Ra dp}) + 6b_1\ (\text{IR, Ra dp}) + 6b_2\ (\text{IR, Ra dp})$$

Although it was not possible to measure the complete vibrational spectra for both isomers, decision between C_{3v} and C_{2v} symmetry for the low-temperature species is facilitated by inspection of the CF (1250–1150 cm^{-1}) and PF (1000–900 cm^{-1}) stretching regions. In the point group C_{3v} the three CF and four PF vibrations transform as (a_1 + e) and ($2a_1$ + e), respectively. Accordingly, for C_{2v} symmetry the vibrations span the representation (a_1 + b_1 + b_2) and ($2a_1$ + b_1 + b_2). Thus, in the CF and PF stretching region, two and three bands respectively, are expected for $PF_4CF_{3,ax}$, and three and four bands respectively, for $PF_4CF_{3,eq}$. Inspection of Tables I and II leaves no doubt that the low-temperature species is $PF_4CF_{3,ax}$. In Figure 1 and 2 bands of the

Table II. Measured and Calculated Fundamental Wavenumbers (cm^{-1}) of $PF_4CF_{3,eq}$

IR spectrum[a]			Raman spectrum			calc[d]		
Ne matrix	Ar matrix	int[b]	liq	int	ρ[c]	value	int (IR)	assignt (C_{2v}); approx descrpn of mode
1238	1235	94				1290	83.9	b_1; $\nu_{as}(CF_3)$
1201	1199	67				1240	33.5	a_1; $\nu_s(CF_3)$
1164.7	1160.9	91				1225	68.7	b_2; $\nu_{as}(CF_3)$
1013.5	1010.4	73				1068	75.5	b_2; $\nu_{as}(PF_{2,eq})$
910.5	906.6	100				1022	100	b_1; $\nu_{as}(PF_{2,ax})$
903	900	81	900			926	88.9	a_1; $\nu_s(PF_{2,eq})$
753.9	755.0	4	671[e]	s	0,4	740	0.5	a_1; $\nu_s(PF_{2,ax})$
673	672.1	8				697	2.7	a_1; $\delta_s(CF_3)$
578.6	576.6	6				530	6.4	
	564.5	7				514	1.0	
	559.6	31				553	62.1	b_1; $\delta_{oop}(PF_{2,eq})$
	534.1	7				503	9.4	
	480.1	10				457	16.6	b_2; $\rho(PF_{2,eq})$
			324	(sh)		318	0.6	a_1; ν(P-CF_3)
			180	m		168	0.2	a_1; $\delta(PF_{2,ax}/PF_{2,eq})$
			105	w		102	0.6	b_2; $\rho(PF_{2,eq}/CF_3)$

[a] Average over matrix splittings. [b] Relative integrated band intensity. [c] Polarization ratio. [d] Ab initio calculations (HF/3-21G*); wavenumbers normalized by a factor of 0.9; further unobserved vibrations are 473, 342, 243, 230, and 28 cm^{-1}. [e] $\delta_s(CF_3)/\nu_s(PF_{2,ax})$, obscured by bands of $PF_4CF_{3,ax}$.

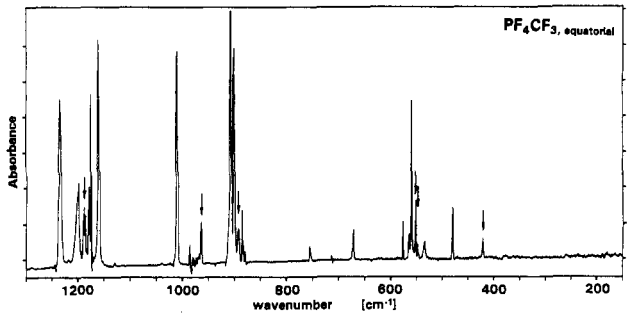

Figure 3. Infrared spectrum of $PF_4CF_{3,eq}$ isolated in an argon matrix, calculated from the spectrum of an equilibrium mixture (sample: Ar = 1:1000; 0.7 mmol matrix) at +120 °C minus that at −125 °C. Arrows indicate bands due to the impurity $PF_2(O)CF_3$.

impurity $PF_2(O)CF_3$ are indicated by arrows. They are located at 1396 (m, br), 1381 (w), 1232.5 (s), 1187 (vs, br), 1180 (vs), 962 (s), 892 (s), 551.5 (s), 547 (m), 422 (m), 308 (w), and 295 (w) cm^{-1}. The identity was confirmed by measurement of the spectrum of a sample of the pure material.

Assignments. Assignment of the vibrational wavenumbers listed in Tables I and II is assisted by comparison with the spectra of PF_5[10] and CF_3SCl,[11] depolarization ratios of the Raman lines, relative band intensities, and vibrational wavenumbers predicted by ab initio calculations.

Stretching Modes of the CF_3 Group. Near 1200 cm^{-1} two and three bands are observed for $PF_4CF_{3,ax}$ (I) and $PF_4CF_{3,eq}$ (II), respectively. The vibrational modes ν_s (CF_3) were assigned according to the polarization ratio of this band in isomer I and the relative IR intensity in isomer II as well as the sequence predicted by ab initio calculations. The mode $\nu_{as}(CF_3)$, which is degenerate in isomer I, is split into two components (b_1 and b_2) in isomer II.

The polarized band at lowest frequency in the Raman spectrum of species I, at 303 cm^{-1}, can be attributed to the P–CF_3 stretching mode, because all other a_1 modes are readily assigned to the PF_4 group. An increase in the temperature causes a shoulder on this Raman band (324 cm^{-1}) of liquid PF_4CF_3 to appear, which is assigned to the corresponding mode of isomer II. This assignment is assisted by the calculated ab initio wavenumbers.

The P–CF_3 stretching modes are remarkable in two respects:

(i) The wavenumber is much lower than the respective S–CF_3 vibration (460 cm^{-1}) in CF_3SCl.[11] A possible explanation is the existence of high positive charges at the C and P atoms, which weaken the P–C bond.

(ii) The wavenumbers for the axial and equatorial CF_3 group are nearly identical although, in general, equatorial bonds are stronger. This observation tallies with the experimental and theoretical structural studies, which deduce very similar P–C bond lengths for the axial and equatorial isomers.

PF_4 Stretching Modes. For the isomer (I) of higher symmetry, two of the four stretching modes are degenerate. This degenerate ν_{as} ($PF_{3,eq}$) vibration is, by analogy with PF_5 (1026 cm^{-1}), the highest PF stretch (985 cm^{-1}) with high infrared and low Raman intensity. The opposite is true for $\nu_s(PF_{3,eq})$, which is observable in the Raman spectrum only (752 cm^{-1}; in PF_5, 817 cm^{-1}). The extremely low infrared intensity indicates a nearly planar $PF_{3,eq}$ skeleton. The remaining PF_{ax} stretch is observed in the infrared and Raman spectra at about 890 cm^{-1}, much higher than the average of ν_s and $\nu_{as}(PF_{2,ax})$ in PF_5 (793 cm^{-1}). In the infrared spectrum of the lower-symmetry isomer (II), all four P–F stretches are observed. Again $\nu_{as}(PF_{2,eq})$ should be the highest mode at about 1010 cm^{-1}, followed by $\nu_{as}(PF_{2,ax})$ at about 910 cm^{-1} (cf. PF_5, 945 cm^{-1}). The corresponding symmetric stretching modes at 900 and 672 cm^{-1} are also observed in the Raman spectrum of liquid PF_4CF_3 at −20 °C, although a low concentration of isomer II is present at this temperature. By analogy with PF_5 ($\nu_s(PF_{2,ax})$ = 640 cm^{-1}), the band at 672 cm^{-1} is assigned to $\nu_s(PF_{2,ax})$. Because this mode is also observed in the infrared spectrum, the $PF_{2,ax}$ group appears to deviate slightly from linearity.

A remarkable splitting is apparent in the band at 980 cm^{-1} (Figure 2). This band displays a similar pattern in a neon matrix, suggesting that this arises from something other than matrix effects. The splitting may be due to coupling of this mode with pseudorotation motions.

Bending Modes. Apart from $\delta_s(CF_3)$, which is expected in the range 780–700 cm^{-1}, all other bending modes occur below the PF and CF stretching vibrations. For isomer I the assignment of $\delta_s(CF_3)$ at 713 cm^{-1} is unambigous, because of its depolarization ratio. In isomer II all bands above 670 cm^{-1} are assigned to stretching modes, and the remaining band at 755 cm^{-1} must be $\delta_s(CF_3)$. For further assignments refer to Tables I and II.

Because the bending modes are strongly hybrid, it is difficult to give a simple description of them, especially for isomer II. The fundamental at 180 cm^{-1} in this isomer is strongly involved in the intramolecular exchange process suggested by Berry.[12] Its wavenumber is lower than the corresponding mode in SF_4 (228

(10) Griffiths, J. E.; Carter, R. P., Jr.; Holmes, R. R. *J. Chem. Phys.* **1964**, *41*, 863; **1965**, *42*, 2632.
(11) Bielefeldt, D.; Willner, H. *Spectrochim. Acta* **1980**, *36A*, 989.
(12) Berry, R. S. *J. Chem. Phys.* **1960**, *32*, 933.

Table III. Results of HF/3-21G* Calculations Including Skeletal Geometric Parameters (pm and deg) for Axial and Equatorial Isomers of PF_4CF_3 and Relative Energies

	axial	equatorial
$P-F_{eq}$	154.7	154.0
$P-F_{ax}$	156.1	157.3[a]
P–C	182.4	182.0
$F_{eq}PF_{ax}$	90.4	90.3[a]
$F_{eq}PF_{eq}$	120.0	118.4
ΔE/kJ mol^{-1}	0.0	−2.72

[a] Mean value.

cm^{-1}),[13] in agreement with the lower barrier for pseudorotation in PF_4CF_3.

Ab Initio Calculations. Calculations on both isomers have been performed at the HF/3-21G* level, using the GAUSSIAN 90 program system.[14] Scaled vibrational wavenumbers and IR intensities are included in Tables I and II and skeletal geometric parameters and relative energies are given in Table III. The fully optimized structure of the equatorial isomer possesses C_2 symmetry with one C–F bond eclipsing an axial P–F bond. The parameters agree very well with the electron diffraction values,[3] except for the P–C bond lengths. The experimental values are considerably longer than the calculated bond lengths ($P-C_{ax}$ = 190.0 (20) vs 182.4 pm, $P-C_{eq}$ = 188.1 (8) vs 182.0 pm). The failure of ab initio calculations with small basis sets to predict $E-CF_3$ bond lengths, where E is a second row element (e.g. $Si-CF_3$, $P-CF_3$ or $S-CF_3$), has been highlighted previously.[15-17] Both experiment and theory, however, result in nearly equal lengths for equatorial and axial P–C bonds. This is quite unusual in trigonal bipyramidal compounds, for which bonding models discussed in the literature[18-20] predict axial bonds to be longer than equatorial bonds. Bond length ratios r_{ax}/r_{eq} between 1.06 and 1.19 have been observed.[20] Nearly equal axial and equatorial P–C bond lengths have also been determined for $(CF_3)_3PCl_2$ ($P-C_{ax}$ = 194.6 (14) pm; $P-C_{eq}$ = 193.8 (31) pm). On the other hand, quite different axial and equatorial bond lengths have been reported for pentaphenylphosphorane[21] ($P-C_{ax}$ = 198.7 pm; $P-C_{eq}$ = 185.0 pm; mean values). These limited structural data indicate that the bonding properties of phosphoranes containing CF_3 groups differ from the models discussed in the literature for pentacoordinated phosphorus compounds. This may explain why (trifluoromethyl)fluorophosphoranes do not obey the electronegativity rule.

Determination of the Equilibrium. As discussed above, the low-temperature (more stable) species is $PF_4CF_{3,ax}$. To evaluate the enthalpy and entropy difference between both isomers, the equilibrium constants for isomerization (1) at different temperatures are required. To this end equilibrium mixtures obtained for different temperatures have been quenched in argon matrices and investigated by infrared spectroscopy. In the temperature-controlled spray-on nozzle (Figure 1) the equilibrium is definitively achieved in each experiment, even at the lowest temperature (−125 °C). This can be concluded from the ^{19}F-NMR experiments at −130 °C where only one signal for the PF_4 group is observed. The exchange frequency between axial- and equatorial-bonded fluorine atoms in the similar but more rigid SF_4 molecule at the coalescence temperature (ca. 20 °C), determined by ^{19}F-NMR spectroscopy, is about 10^4 s^{-1}.[22] Because the coalescence temperature for PF_4CF_3 is below −130 °C, the time for achievement of the equilibrium between the PF_4CF_3 isomers at this temperature is several orders of magnitude shorter than the residence time of the Ar/PF_4CF_3 mixture in the spray-on nozzle (≈5 s, see Experimental Section).

Table IV. Results for Determination of Equilibrium Constants

	sum of absorbances[a]			
temp/K	$PF_4CF_{3,equatorial}$	$PF_4CF_{3,axial}$	K_p[a]	ln K_p
149	3.779	24.584	0.1894	−1.664
188	6.005	17.673	0.4187	−0.871
254	12.428	17.971	0.8521	−0.160
295	14.464	16.186	1.1010	0.096
295	11.379	12.730	1.1014	0.097
296	12.515	14.427	1.0688	0.067
353	13.610	11.400	1.4710	0.386
379	17.033	13.194	1.5906	0.464

[a] See text.

It is assumed that the equilibrium is not disturbed by the quenching process in the argon matrix like in several similar studies on rotational conformers[23] and in the recent example of (fluorocarbonyl)sulfenyl chloride.[24] This fundamental assumption is correct for the studied PF_4CF_3 system because the ratio of isomers at room temperature is the same in the electron diffraction study.[3]

In the infrared spectrum of an equilibrium mixture one can see several bands of both isomers which occur in regions district from each other. These occur for $PF_4CF_{3,ax}$ at 1244, 979, 885, 712, and 576 cm^{-1} and for $PF_4CF_{3,eq}$ at 1199, 1161, 1010, 907, 900, and 672 cm^{-1}. The sum of integrated absorbances of these bands (see Table IV) have been used to determine the equilibrium constants. Because the ratio of both sums of absorbances is not equivalent to the molar ratio, one has to determine the proportionality factor. For this, the sum of absorbances for both isomers at different temperatures have been determined, normalized to the same amount of PF_4CF_3 (2 μmol). The amount of PF_4CF_3 was deduced from the amount of matrix deposited and from the absorbance of the tracer $PF_2(O)CF_3$. The result is

$$\frac{\text{decrease of absorbance } PF_4CF_{3,eq}}{\text{increase of absorbance } PF_4CF_{3,ax}} = 0.81 \pm 0.08$$

i.e., the selected bands of $PF_4CF_{3,eq}$ are weaker. To convert the absorbance ratio into a molar ratio (K_p, Table IV), the sum of absorbances of $PF_4CF_{3,ax}$ has to be multiplied by 0.81.

The differences in enthalpy and entropy of both isomers were evaluated by the method of van't Hoff and Ulich:

$$-\ln K_p = \Delta H^\circ (RT)^{-1} - \Delta S^\circ (R)^{-1} \qquad (2)$$

Data from Table IV lead to Figure 4 and finally to

$$\Delta H^\circ = 4.32 \pm 0.05 \text{ kJ mol}^{-1}$$
$$\Delta S^\circ = 15.4 \pm 1.0 \text{ J mol}^{-1} \text{ K}^{-1}$$

averaged over the temperature range used. The uncertainty in ΔH° is due mainly to errors in determination of the temperature and of K_p; that for ΔS° is due to the error in the proportionality factor.

(13) Christe, K. O.; Willner, H.; Sawodny, W. *Spectrochim. Acta* **1979**, *35A*, 1347.
(14) Frisch, M. J.; Head-Gordon, H.; Trucks, G. W.; Foresman, J. B.; Schlegel, H. B.; Raghavachari, K.; Robb, M.; Binkley, J. S.; Gonzalez, C.; DeFrees, D. J.; Fox, D. J.; Whiteside, R. A.; Seeger, R.; Melius, C. F.; Baker, J.; Martin, R. L.; Kahn, L. R.; Stewart, J. J. P.; Topiol, S.; Pople, J. A. Gaussian 90, Revision F. Gaussian Inc., Pittsburgh, PA, 1990.
(15) Marsden, C. J. *Inorg. Chem.* **1984**, *23*, 1703.
(16) Magnusson, E. *J. Am. Chem. Soc.* **1986**, *108*, 11.
(17) Rempfer, B.; Pfafferott, G.; Oberhammer, H.; Beckers, H.; Bürger, H.; Eujen, R.; Boggs, J. E. *Rev. Chim. Miner.* **1986**, *23*, 551.
(18) Craig, D. P.; Maccoll, A.; Nyholm, R. S.; Orgel, L. E.; Sutton, L. E. *J. Chem. Soc.* **1954**, 332.
(19) Rundle, R. E. *Rec. Chem. Prog.* **1962**, *23*, 195.
(20) Gillespie, R. J. *Molecular Geometry*; Van Nostrand Reinhold: London, 1972. Gillespie, R. J.; Hargittai, I. *The VSEPR Model of Molecular Geometry*; Allyn and Bacon: Boston, MA, 1991.
(21) Wheatley, P. J. *J. Chem. Soc.* **1964**, 2206.
(22) Seel, F.; Gombler, W. *J. Fluorine Chem.* **1974**, *4*, 327. Gombler, W. Private communication 1992.
(23) Barnes, A. J. In *Matrix Isolation Spectroscopy*; Barnes, A. J., Orville-Thomas, W. J., Müller, A., Gaufrés, R., Eds.; NATO ASI, Series C; Reidel Publ.: Dordrecht, Holland, 1981; Vol. 76.
(24) Mack, H. G.; Oberhammer, H.; Della Védova, C. O. *J. Phys. Chem.* **1991**, *95*, 4238.

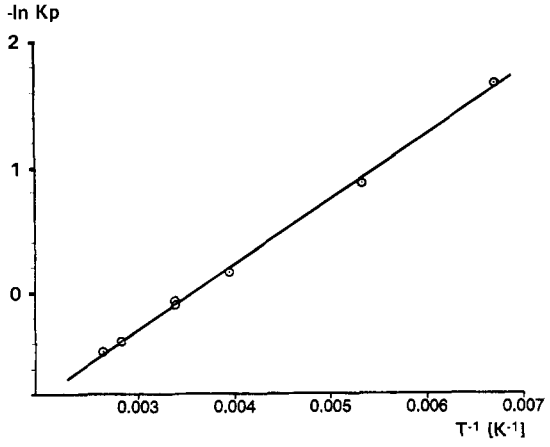

Figure 4. Van't Hoff plot for the equilibrium $PF_4CF_{3,ax} \rightleftharpoons PF_4CF_{3,eq}$.

The proportion of the less stable isomer, $PF_4CF_{3,eq}$, in the equilibrium at −100, +22, and +100 °C is 24, 53, and 61%, respectively. In the electron diffraction study at room temperature, 60 ± 10% of $PF_4CF_{3,eq}$ was found,[3] which is in excellent agreement with the present results.

The difference in the enthalpies is surprisingly low. To our knowledge, no other phosphorane is known for which axial and equatorial isomers exist simultaneously. The ab initio calculations predict the equatorial isomer to be slightly more stable (ΔE = −2.72 kJmol^{-1}), in contrast to the matrix isolation experiment which indicates in a preference for the axial form ($\Delta H°$ = +4.32 (5) kJ mol^{-1}). Considering the low level of these calculations (Hartree–Fock approximation and small basis sets) for describing the complex bonding situation in hypervalent compounds, this discrepancy of ca. 7 kJ mol^{-1} is not unexpected.

Because the P–C bond lengths (see above) and the bond strengths (ν(P–CF_3) equatorial: 324 cm^{-1}, axial: 303 cm^{-1}) are very similar, one can conclude also that the bond energies may be nearly equal. Hence the low enthalpy difference is due mainly to the difference in the bond energies of PF_{ax} and PF_{eq}, which should be small as indicated by their rather similar lengths (see Table III).

On the other hand, the entropy difference between the two isomers is surprisingly high. A deeper understanding of this large difference is obtained from a statistical thermodynamical analysis. From rotational constants and vibrational wavenumbers (Tables I and II), entropy values $S°_{298}$ of 373.1 and 387.2 J mol^{-1} K^{-1} are calculated for the axial and equatorial conformer respectively. The difference $\Delta S°_{298}$ = 14.1 J mol^{-1} K^{-1} is in good agreement with the experimental value. The main contributions to the large entropy difference come from the symmetry number (axial, σ = 3; equatorial, σ = 1) in the rotational term and from the great difference in the torsional frequencies (τ(CF_3): axial, 77 cm^{-1}; equatorial, 28 cm^{-1}) in the vibrational term.

Acknowledgment. Support by the Deutsche Forschungsgemeinschaft (DFG), and Fonds der Chemischen Industrie is gratefully acknowledged.